NASA TM-84236

Adaptive-Wall Wind-Tunnel Research at NASA-Ames Research Center

Edward T. Schairer and Joel P. Mendoza

May 1982

NASA
National Aeronautics and
Space Administration

N82-24214

Adaptive-Wall Wind-Tunnel Research at NASA-Ames Research Center

Edward T. Schairer
Joel P. Mendoza, Ames Research Center, Moffett Field, California

N82-24214

ADAPTIVE-WALL WIND-TUNNEL RESEARCH AT AMES RESEARCH CENTER

Edward T. Schairer and Joel P. Mendoza
Ames Research Center, Moffett Field, California 94035, U.S.A.

SUMMARY

Adaptive-wall wind-tunnel research conducted at Ames Research Center, NASA, is summarized. This research includes small-scale two-and three-dimensional wind-tunnel experiments and numerical experiments with a three-dimensional adaptive-wall simulator. In the two-dimensional experiment, an NACA 0012 airfoil was tested in a 25- by 13-cm slotted-wall test section. Airflow through the test-section walls was controlled by adjusting the pressures in segmented plenums. Interference-free conditions were successfully attained in subsonic and transonic flows. Based on the design of this small-scale test section, an adaptive-wall test section is being constructed for the 2- by 2-Foot Transonic Wind Tunnel at Ames. For the three-dimensional experiment, the 25- by 13-cm wind tunnel was modified to permit cross-stream wall adjustments. The test model was a semispan wing mounted to one sidewall. Wall interference was substantially reduced at several angles of attack at Mach 0.60. A wing-on-wall configuration was also modeled in the numerical experiments. These flow simulations showed that free-air conditions can be approximated by adjusting boundary conditions at only the floor and ceiling of the test section. No sidewall control was necessary. Typical results from these experiments are discussed.

SYMBOLS

b	wing semispan, cm
c	wing chord, cm
$\bar{c}$	wing mean aerodynamic chord, cm
C_L	lift coefficient
C_p	pressure coefficient
M	Mach number
R	Reynolds number
U_∞	longitudinal free-stream velocity, m/sec
w	vertical velocity, m/sec
x	longitudinal direction, positive downstream, measured from airfoil leading edge in two-dimensional experiments, and from wing quarter chord in three-dimensional experiments, cm
y	spanwise direction, positive outboard of wing root, cm
z	vertical direction, positive above wing, cm
α	angle of attack, deg

INTRODUCTION

Wind tunnels with walls that can be adjusted to eliminate wall interference were demonstrated in England during World War II (Refs. 1-3). These wartime experiments were motivated by the need to reduce blockage interference and eliminate choking in transonic wind tunnels. This was accomplished by bending the tunnel floor and ceiling to conform to free-air streamlines. Although the British experiments were successful, calculations of the streamline shapes were laborious, and a separate computation was required for each combination of model, model attitude, and free-stream condition. After the War, the emphasis of British wind-tunnel research was switched to the development of ventilated-wall test sections.

Recent papers by Ferri and Baronti (Ref. 4) and Sears (Ref. 5) have stimulated new interest in developing adjustable-wall wind tunnels. Ferri and Sears showed that wall interference can be estimated based on measured flow conditions alone, without any knowledge of the model. This insight has greatly simplified the problem of determining the wall adjustments needed to produce interference-free flow. Furthermore, the calculation of free-air conditions can be performed on-line with small contemporary computers. Thus, the prospects for developing practical adaptive-wall wind tunnels are much better today than they were 40 years ago.

Interest in adaptive-wall wind tunnels has also been renewed because flight conditions of modern aircraft are becoming increasingly difficult to simulate in conventional wind tunnels without significant wall interference. In complicated flow problems, analytically "correcting" wind-tunnel data for wall interference is, at best, very difficult. Avoiding excessive wall interference by testing small models in relatively large test sections comes at the expense of Reynolds number simulation. In addition, this approach makes inefficient use of the airstream and may become prohibitively costly as wind tunnels become more expensive to operate.

An adaptive-wall wind tunnel alleviates wall interference by utilizing capabilities of both the tunnel and a computer. The wind tunnel represents the flow near the model which, because of its complexity, cannot be adequately simulated numerically. The computer economically predicts the unconfined far-field flow, which is relatively simple. Tunnel-wall conditions are adjusted until conditions at the interface between the near-field flow (wind tunnel) and far-field flow (computer) are compatible.

The objective of adaptive-wall wind-tunnel research at Ames Research Center is to develop test sections in which unconfined two- and three-dimensional transonic flows can be simulated. To be practical, the procedures for eliminating wall interference must be fast, accurate, reliable, and automatic. The research program consists of parallel experimental and theoretical studies. The experimental program began with small-scale two- and three-dimensional tests. These tests have been completed, and a summary of these results is presented in this paper. The next major step in the experimental program will be a demonstration of a two-dimensional adaptive-wall test section in the Ames 2- by 2-Foot (0.61- by 0.61-m) Transonic Wind Tunnel. The test section is under construction and operation is scheduled for the Spring of 1983.

The operation of adaptive-wall wind tunnels was simulated using numerical models. Among the configurations studied was the small-scale three-dimensional adaptive-wall wind tunnel as described in this paper. Typical results are presented here.

Adaptive-wall research at Ames has focused on slotted-wall test sections in which airflow through the walls is controlled by adjusting the pressures in plenum compartments. This approach was selected primarily because of the wide use of slotted-wall test

sections at Ames. In addition, a subdivided plenum allows for simultaneous adjustment of wall conditions in both streamwise and cross-stream directions, as is required in a three-dimensional adaptive-wall test section. Finally, slotted walls, as opposed to perforated walls, provide space between the slots, permitting the use of nonintrusive, optical measurement techniques.

ADAPTIVE-WALL PROCEDURE

The adaptive-wall procedure used in the Ames studies was conceived by Davis (Ref. 6) and is a modification of Sears' approach (Ref. 5). Whereas Sears predicts free-air conditions by measuring two different flow quantities on one surface surrounding the model, Davis's method requires that only one flow quantity be measured on two surfaces. This can significantly simplify the experimental problem.

Figure 1 illustrates schematically Davis's adaptive-wall procedure applied to the special case of two-dimensional, symmetric flow. In this case, the two surfaces surrounding the model can be reduced to two parallel lines extending infinitely far upstream and downstream. Flow past the model is divided into two regions: a near-field region between the model and the outer line (field level), and a far-field region extending from the inner line (source level) to infinity. In the wind-tunnel experiment, the near-field region is represented by the flow past the model in the wind tunnel; in computer simulations, this flow is represented numerically. In both the wind-tunnel tests and the simulations, the far-field region is represented by a theoretical model of unconfined flow.

The first step in the adaptive-wall procedure (Fig. 1) is to determine the distribution of some flow quantity along the source and field lines in the near-field region. In the present studies, vertical velocity (upwash) was the chosen flow quantity because it is a perturbation quantity which can be easily measured with a laser velocimeter. The measured upwash at the source level is used as one boundary condition in the theoretical representation of the outer-flow region. At the other (far-field) boundaries, free-air conditions are imposed (perturbations vanish at infinity). The corresponding free-air distribution of vertical velocity at the field level is then computed ("outer-flow solution") and compared with the actual distribution determined experimentally (in the wind tunnel) or numerically (in the computer simulation). Differences between the actual and free-air velocity distributions at the field level are due to wall interference and are used as a basis for adjusting the flow conditions at the wind-tunnel walls. In the wind-tunnel experiments, wall conditions were changed by adjusting the airflow through the slotted walls. In the numerical simulation, wall adjustments were made by imposing normal velocity boundary conditions at panels simulating the test-section walls. Since wall adjustments change the conditions at the source level, the adaptive-wall procedure is repeated until the actual and free-air vertical velocity distributions at the field level converge.

SMALL-SCALE EXPERIMENTS

Small-scale two- and three-dimensional adaptive-wall experiments were performed in the Ames 25- by 13-cm Indraft Wind Tunnel (Fig. 2). The model for the two-dimensional experiment was a NACA 0012 airfoil; in the three-dimensional experiment, the model was a semispan wing mounted on one of the sidewalls of the test section. For both experiments, the test section had slotted upper and lower walls and solid plexiglas sidewalls. Separate top and bottom plenums were divided into compartments, and the pressure in each compartment was independently adjustable. In the two-dimensional experiment, the compartments were arranged longitudinally with each compartment spanning the width of the test section (Fig. 3). The compartments nearest the model were smaller than upstream and downstream compartments because velocity gradients near the model were expected to be large. The three-dimensional test section had the same longitudinal arrangement of compartments, but each of the six upper and lower compartments closest to the model was subdivided into three cross-stream compartments.

Laser velocimetry (LV) was used to measure vertical velocities at control points on the source and field surfaces (Fig. 4). The velocimeter could traverse in the streamwise and vertical directions, and measurements were made at the midspan station for the two-dimensional tests. For the three-dimensional experiment, the velocimeter could, in addition, traverse in the spanwise direction. Motion of the velocimeter, data acquisition, and data reduction were automatically controlled on-line, using a dedicated minicomputer.

Interference-free velocities at the field-level control points were predicted using linear compressible flow theory. The two-dimensional problem was solved analytically (Ref. 6); however, an approximate, finite-difference solution was necessary for the three-dimensional problem. In both cases, the solutions were computed on-line and displayed graphically. The solution required several seconds of computation time for the two-dimensional problem and about 30 sec for the three-dimensional case. The computer speed was about 0.5 million floating point operations per second (MFLOPS).

Pressure adjustments in the plenum compartments were computed from influence coefficients which had been empirically determined in the empty test section before the experiments. Each influence coefficient represented the change in vertical velocity at a control point on the field surface produced by a unit change in pressure in one plenum compartment. The influence-coefficient matrix was inverted and multiplied by desired velocity changes at the field level to determine required plenum pressure changes.

Each plenum compartment was connected to high- and low-pressure air reservoirs by means of flexible plastic hose, PVC pipe, and two ball valves (Fig. 2). Twenty such channels of air were required for the two-dimensional experiment, and 36 for the three-dimensional test. A pressure change in a particular plenum compartment was produced by manually adjusting the appropriate ball valve.

Two-Dimensional Experiments

The NACA 0012 airfoil in the adaptive-wall test section is illustrated in Fig. 3. The height-to-chord ratio of the model in the test section was 1.66, and static pressure orifices were located its upper and lower surfaces. The experiments were conducted at Mach numbers between 0.6 and 0.8 and at angles of attack of 0° and 2°.

Figure 3 also illustrates the points at which upwash was measured at the source and field levels. The source levels were located just beyond optical obstructions produced by the model supports. The field levels were located far enough away from the tunnel walls to avoid the boundary layer and three-dimensional perturbations produced by individual slots.

The adaptive-wall procedure converged to free-air conditions when the supersonic zone on the upper surface of the airfoil remained below the source level. This conclusion is based on a comparison of the measured velocities at the field-level control points with the

free-air velocities predicted by the outer-flow solver. The conclusion was corroborated by comparing the pressure distribution measured across the chord of the airfoil with interference-free pressure data (Ref. 7).

Figure 5 illustrates a sample case (Mach 0.78, $\alpha = 0°$) in which free-air conditions were successfully approximated. The figure shows field-level velocities and model pressure distributions before and after plenum pressures were adjusted. Because the flow was symmetric at an angle of attack of $0°$, velocity measurements were only made at the source and field levels above the airfoil. The top and bottom walls were adjusted symmetrically. Before the walls were adjusted, there were significant differences between the measured velocity distribution at the field level and the free-air distribution predicted by the outer flow solver. The shock wave position, evident from the pressure data, was downstream of its free-air location (Ref. 7). After three cycles of wall adjustments, both the velocity and pressure distributions were in much better agreement with the free-air data.

When the supersonic zone extended beyond the source level (for example, Mach 0.8, $\alpha = 2°$), the adaptive-wall procedure did not converge on unconfined flow. This was partly because linear theory was used to predict free-air velocities at the field level. In addition, the 25- by 13-cm Wind Tunnel could not produce steady free-stream flow at this condition. Nonlinear solutions to the outer flow problem are being developed and will be available when the 2- by 2-foot adaptive-wall test section becomes operational. Further details of the two-dimensional experiment are given in Ref. 8.

Three-Dimensional Experiments

The test section for the three-dimensional adaptive-wall experiment is illustrated schematically in Fig. 6. The model was an unswept, untwisted, tapered wing semispan. The airfoil (NACA 65A006) was constant from root to tip. The wing is a replica of a model tested at Langley in 1951 as part of a program to investigate the interference characteristics of ventilated-wall test sections (Ref. 9). This model was selected for the adaptive-wall experiment because free-air data were available from Ref. 9. The ratio of the test-section height to the wing mean aerodynamic chord ($\bar{c}$) was 1.5, and the ratio of the test-section width to the wing semispan was 1.47. The model was constructed of solid stainless steel and was supported by a balance that provided force and moment data.

Figure 7 is a cross-sectional view of the test section showing the source and field surfaces and the locations at which LV measurements were made. Vertical velocities were measured at seven such cross sections, beginning 1.15 $\bar{c}$ upstream and ending 1.15 $\bar{c}$ downstream of the wing quarter chord. Acquisition and reduction of the LV data required 20 min.

The adaptive-wall experiments were performed at Mach 0.60 and at angles of attack between $0°$ and $6°$. In all of the experiments, wall interference was substantially reduced after the wall boundary conditions had been adjusted according to the adaptive-wall procedure. This finding is supported by several comparisons of data from the experiment with free-air data. First, the vertical velocities measured at the field surface were compared with the free-air velocities predicted by the outer flow solver. In addition, the measured vertical velocities were compared with velocities predicted by numerical simulation of the model in unconfined flow. Finally, the change in lift coefficient produced by the wall adjustments indicates a reduction in wall interference.

Figure 8 illustrates vertical velocity data along two longitudinal lines at the field surface at Mach 0.6, $\alpha = 5.3°$. (The insets illustrate the positions of the lines where measurements were made relative to the model.) Data labeled "passive wall" were measured before the wall boundary conditions were adjusted. The "adapted wall" data were measured after two cycles of wall adjustments. The "outer-flow solution" is the estimate of free-air conditions made after the second cycle of wall adjustments. The figure shows that differences between the measured data and the outer-flow solution were smaller after the walls were adjusted, indicating a reduction in wall interference. Similar reductions occurred at other locations on the field surface. The corresponding change in the lift coefficient of the model is illustrated in Fig. 9. The figure also includes interference-free data from the Langley experiments (Ref. 9).

Vertical velocities for another flow condition (Mach 0.6, $\alpha = 2°$) are illustrated in Fig. 10. The top half of the figure compares the passive wall upwash with (1) the free-air upwash predicted by the outer flow solution and (2) the upwash determined by numerical simulation of the wing in unconfined flow. The bottom half of the figure shows the effects of three cycles of wall adjustments. Differences between the measured upwash, the outer-flow solution, and the unconfined-flow solution were substantially smaller after the walls were adjusted.

It is evident in Figs. 8-10 that wall interference was not eliminated after the last cycle of wall adjustments. One reason was that the outer-flow solver underpredicted the velocity changes required to match free-air conditions. Another factor was that the required velocity changes at the field surface could not be accurately produced. This was due to the complex flow through the slotted walls and to the over-simplified influence coefficient method used to represent it. Also contributing to the residual errors was the inability to control the velocity distribution on the vertical face of the field surface outboard of the wing tip. Interference errors on this face, however, were small compared with the initial errors on the other faces. Finally, the maximum available suction in several plenum compartments was not sufficient to produce the required pressure changes. Further details of the three-dimensional experiment will be published in the near future.

2- BY 2-FOOT ADAPTIVE-WALL TEST SECTION

An adaptive-wall test section for the 2- by 2-Foot Transonic Wind Tunnel is under construction. This test section is designed to demonstrate the practical application of adaptive-wall technology to two-dimensional transonic testing. The design of the test section (Fig. 11) is similar to that of the test section used in the small-scale experiments; however, it includes several important improvements. Flow through the slotted walls will be controlled by 64 slide valves, each driven by a stepping motor and controlled by a small computer. Ultimately, wall adjustments will be made automatically without intervention by the tunnel operator. As in the small-scale experiment, laser velocimetry will be used to measure vertical velocities in the test section. A very fast, computer-controlled traverse system is being developed which will substantially reduce LV data acquisition times. A nonlinear outer-flow solver is being developed to estimate free-air conditions when there are supersonic zones in the outer region. The solution will be computed by a minicomputer coupled to an array processor.

NUMERICAL SIMULATION

The operation of three-dimensional adaptive-wall wind tunnels was simulated numerically, using both a linear-panel flow code (Ref. 10) and a transonic potential-flow code (FLO29) (Ref. 11). The primary objective of the numerical simulations was to demonstrate convergence of the adaptive-wall procedures to free-air conditions or to demonstrate alternative methods for establishing interference-free conditions in the test section or both. An additional objective was to study the placement of plenum compartments and to establish the number of compartments required to eliminate wall interference.

One of the configurations modeled using the linear code was the semispan wing in the 25- by 13-cm adaptive-wall test section (Fig. 12). The floor and ceiling panels near the wing corresponded to the locations of plenum compartments. Far upstream and downstream of the wing, the floor and ceiling were solid. The inboard sidewall, being a plane of symmetry, was assumed to be solid. Simulations were performed assuming both a solid and an adjustable outboard sidewall. Adjustments to the outboard sidewall were simulated by imposing normal (cross-flow) boundary conditions at the wall panels near the wing.

Conditions for the numerical simulations were Mach 0.60 and $\alpha = 2°$. The simulations began with solid-wall boundary conditions. Figure 13a compares the solid-wall upwash along one line at the field surface with the free-air velocities predicted by the outer-flow solver and with the true free-air upwash. The outer-flow solution under-estimated the velocity changes needed to match free-air conditions; however, the directions of the changes were correct.

The effects of one cycle of wall adjustments are illustrated in Fig. 13b. Boundary conditions at the walls, including the outboard sidewall, were adjusted so that velocities at the field surface approximately matched the outer-flow solution. These adjustments reduced the differences between the actual (adapted wall) and free-air upwashes and decreased the lift coefficient to a value closer to the free-air value. A new outer-flow solution called for additional velocity changes which would have further improved the agreement with the free-air data. Without systematic overcorrection of the walls, however, the rate of reduction of wall interference would be quite slow. Additional cycles of the adaptive-wall procedures were not attempted.

The numerical flow simulation studies were also used to demonstrate that if the actual free-air vertical velocity distributions at the field surface were known in advance, then the boundary conditions at the panels of the floor and ceiling of the wind tunnel could be adjusted so that velocities at the field surface would match the free-air velocities. Free-air velocities, rather than being successively approximated by the outer-flow solver, were calculated directly using the linear code. At the floor and ceiling panels, boundary conditions were adjusted so that velocities at field-surface control points matched the free-air velocity distributions at the field surface. The agreement between the free-air and adapted-wall velocity data is quite good. The adapted-wall lift coefficient also agrees well with the free-air value.

The numerical simulations demonstrated that for a wing-on-wall configuration, free-air conditions can be approximated by adjusting only floor and ceiling panels and not the sidewalls. These results provided the basis for the arrangement of plenum compartments in the 25- by 13-cm wind tunnel. The same result was obtained for a different wing-on-wall configuration simulated using the FLO29 code.

The numerical simulations also demonstrated the advantage of directly computing free-air conditions. Wall adjustments can be made in one step, instead of many steps, as required if the iterative adaptive-wall procedure is used. The direct method may be applicable to configurations where the model and flow near the model are amenable to numerical simulation. However, for complex models or flows, numerical simulation may not be possible. These complex flows are of paramount interest precisely because they cannot be modeled numerically. Details of the numerical studies will be published in the near future.

CONCLUDING REMARKS

A program of combined numerical and wind-tunnel experiments has shown that two- and three-dimensional unconfined flows can be simulated in adaptive-wall test sections. At the same time, a number of issues have been identified that will be the subjects of future research.

The small-scale two-dimensional experiments showed that a slotted-wall wind tunnel with a subdivided plenum can be used to produce interference-free flow in those cases in which the supersonic bubble is not too large. Where stronger shock waves with extensive regions of supercritical flow exist, the basic technique must be augmented with a nonlinear outer-flow solver. This capability will be included in the new 2- by 2-Foot Adaptive Wall Wind Tunnel now under construction. The small-scale three-dimensional experiments were compromised because velocity changes required to eliminate wall interference could not be accurately produced. Further small experiments are planned to examine plenum pumping requirements and the relation between plenum pressures and test-section velocities.

Numerical simulation of the wing-on-wall experiment showed that one cycle of the adaptive-wall procedure reduced wall interference. Although convergence of the procedure to free-air conditions was not demonstrated, the rate of reduction of wall interference appeared to be slow. Convergence will be investigated in the future. An alternative procedure, involving direct computation of free-air flow past the model, was successfully demonstrated. This is reminiscent of the approach used in the British wartime experiments. The direct approach may now be practical for simple configurations (for example, attached flow past an airfoil) because of progress in computational aerodynamics. For more complex flow problems, the direct approach could provide a good first approximation of wall adjustments needed to produce free-air flow. The adaptive-wall procedure could then be applied to eliminate residual interference.

REFERENCES

1. Preston, J.; and Sweeting, N.: The Experimental Determination of the Interference on a Large Chord Symmetrical Joukowski Aerofoil Spanning a Closed Tunnel, Aeronautical Research Committee, R&M No. 1997, Dec. 1942.

2. Preston, J.; Sweeting, N.; and Cox, D.: The Experimental Determination of the Two-Dimensional Interference on a Large Chord Piercy 12/40 Aerofoil in a Closed Tunnel Fitted with a Flexible Roof and Floor, Aeronautical Research Committee, R&M No. 2007, Sept. 1944.

3. Lock, C.; and Beavan, J.: Tunnel Interference at Compressible Speeds Using Flexible Walls of a Rectangular High Speed Tunnel, Aeronautical Research Committee, R&M No. 2005, 1944.

4. Ferri, A.; and Baronti, P.: A Method for Transonic Wind Tunnel Corrections, AIAA J., vol. 11, Jan. 1973, pp. 63-66.

5. Sears, W. R.: Self-Correcting Wind Tunnels, Calspan Report No. RK-5070-A-2, July 1973; also Aeronaut. J., vol. 78, Feb.-Mar. 1974, pp. 80-89.

6. Davis, S.: A Compatibility Assessment Method for Adaptive-Wall Wind Tunnels, AIAA J., vol. 19, Sept. 1981, pp. 1169-1173.

7. Vidal, R. K.; Catlin, P. A.; and Chudyk, D. W.: Two-Dimensional Subsonic Experiments with a NACA 0012 Airfoil, Calspan Report RK-5070-A-3, Dec. 1973.

8. Satyanarayana, B; Schairer, E.; and Davis, S.: Adaptive-Wall Wind Tunnel Development for Transonic Testing, J. Aircraft, vol. 18, no. 4, Apr. 1981.

9 Sleeman, W.; Klevatt, P.; and Linsley, E.: Comparison of Transonic Characteristics of Lifting Wings from Experiments in a Small Slotted Tunnel and the Langley High-Speed 7- by 10-Foot Tunnel, NACA RM L51F14, Nov., 1951.

10. Hess, J. L.: Calculation of Potential Flows about Arbitrary Three-Dimensional Lifting Bodies, Douglas Aircraft Co., Inc., Report MDC-J5679-01, Oct. 1972.

11. Mercer, J.; Geller, E.; Johnson, M.; and Jameson, A.: A Computer Code to Model Swept Wings in an Adaptive Wall Transonic Wind Tunnel, AIAA Paper 80-0156, Pasadena, Calif., Jan. 14-16, 1980.
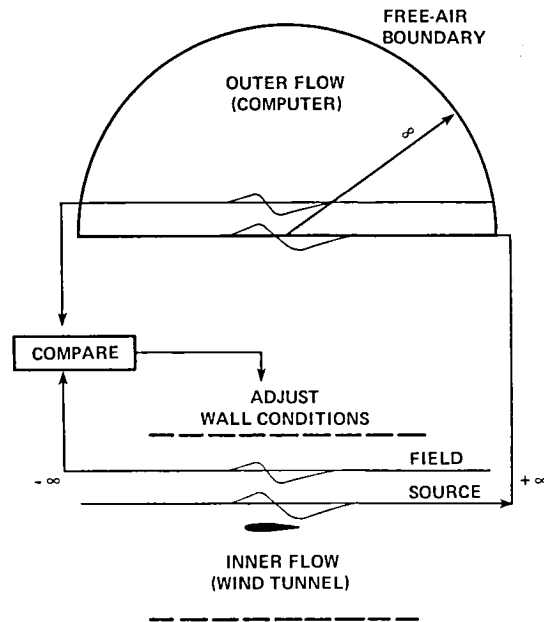
6

FREE-AIR
BOUNDARY

OUTER FLOW
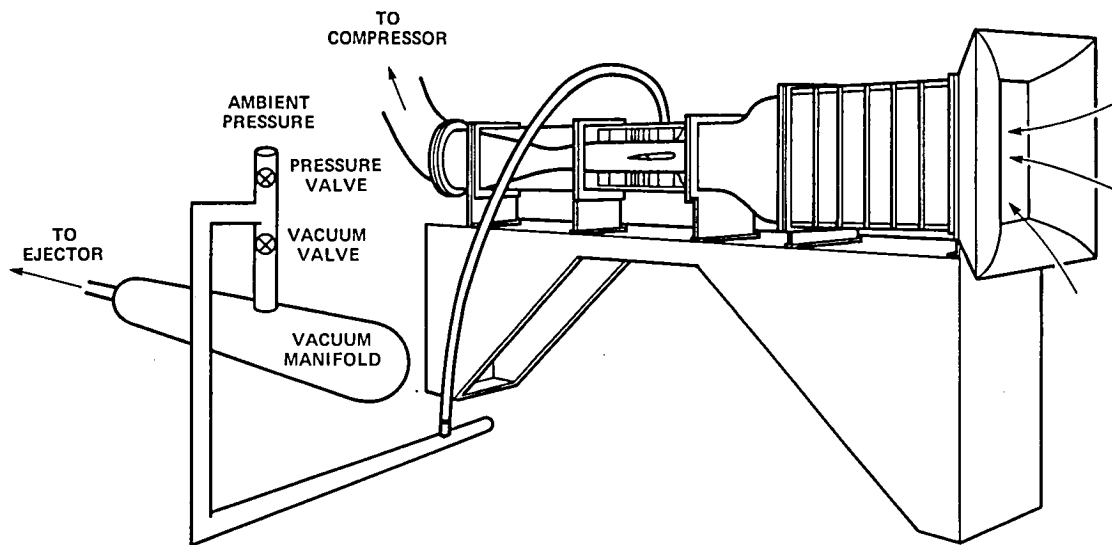(COMPUTER)

∞

COMPARE

ADJUST
WALL CONDITIONS

FIELD

SOURCE

- ∞   + ∞

INNER FLOW
(WIND TUNNEL)

Fig. 1. Adaptive-Wall Procedure

TO
COMPRESSOR

AMBIENT
PRESSURE

PRESSURE
VALVE

VACUUM
VALVE

TO
EJECTOR

VACUUM
MANIFOLD

Fig. 2. 25- by 13-cm Adaptive-Wall Wind Tunnel

2.54 cm

13 cm

FIELD

SOURCE

+ + + + + + + +
+ + + + + + + + + + + +
+ + + + + + + + + + + +
+ + + + + + + +

73.6 cm

Fig. 3. Two-Dimensional Adaptive-Wall Test Section

TEST SECTION

COLLECTING LENS

PHOTO-DETECTOR

TRANS-MITTING LENS

LASER

LASER BEAM

BRAGG CELL

CUBE

COLLECTING OPTICS

TRANSMITTING OPTICS

Fig. 4. Laser Velocimeter

8

INITIAL   FINAL
                    FIELD LEVEL UPWASH

                    □   LASER VELOCIMETER DATA
                    ──●── OUTER FLOW SOLUTION

AIRFOIL PRESSURE DISTRIBUTION

ADAPTIVE-WALL
$M = 0.78$, $R = 10^6$, $\alpha = 0°$

□   UPPER SURFACE
◰   LOWER SURFACE

──●── FREE-AIR (REF 7)
$M = 0.8$, $R = 10^6$, $\alpha = 0°$

Fig. 5.   Two-Dimensional Adaptive-Wall Data
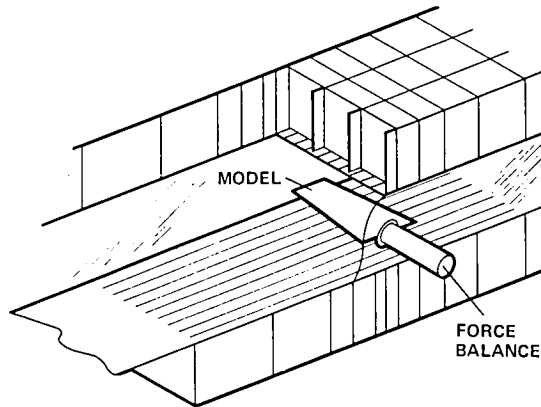
Fig. 6.   Three-Dimensional Adaptive-Wall Test Section

9
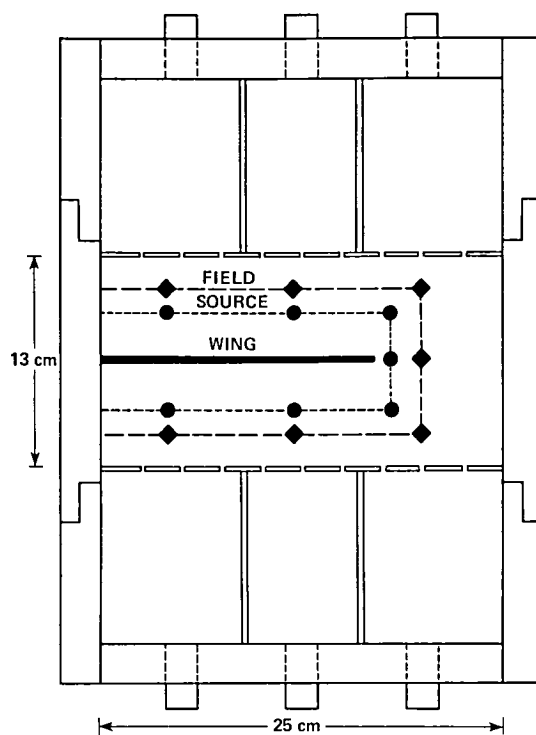
Fig. 7. Laser Velocimeter Measurement Locations
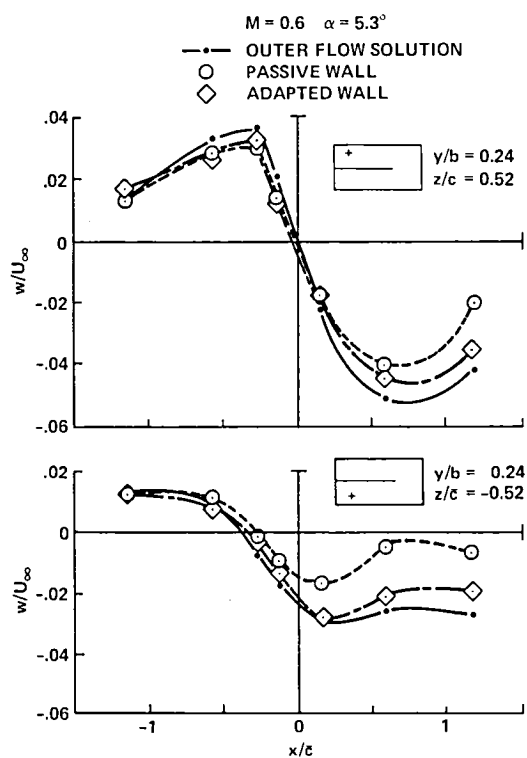
Fig. 8. Effect of Adaptive-Wall Procedure on Upwash Distribution

M = 0.60
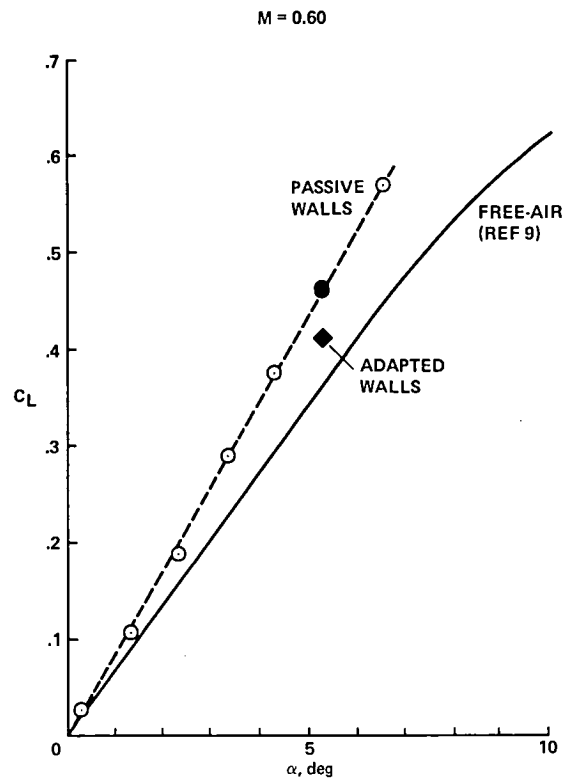
Fig. 9.   Effect of Adaptive-Wall Procedure on Lift Coefficient

M = 0.60 $\alpha = 2°$
—✕— FREE-AIR
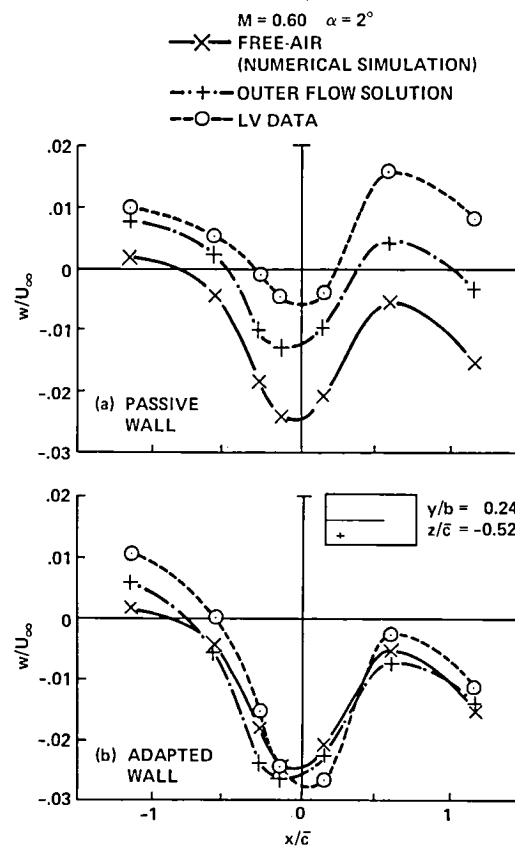(NUMERICAL SIMULATION)
—·+·— OUTER FLOW SOLUTION
——O—— LV DATA

Fig. 10.   Comparison of Measured Upwash with Outer Flow Solution and Numerical Simulation
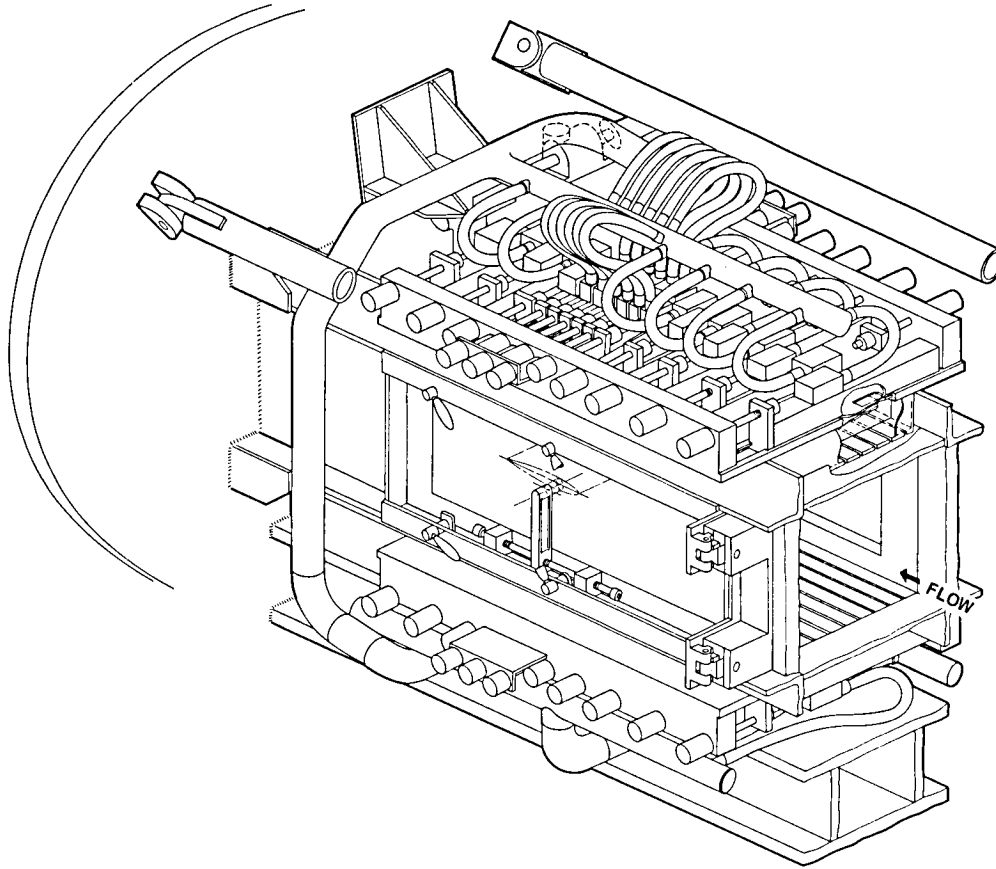
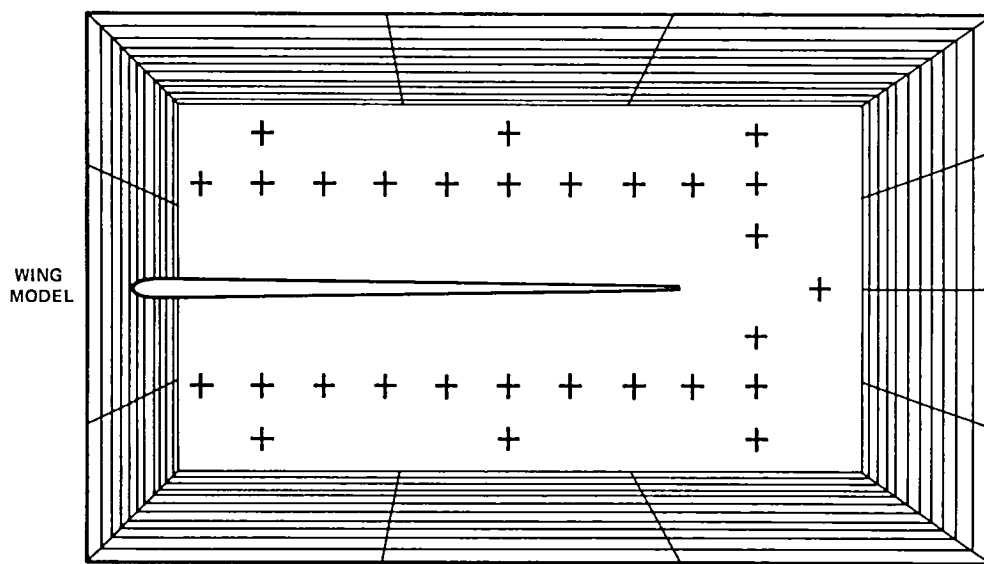Fig. 11.   Two-by-Two Foot Transonic Wind Tunnel Adaptive-Wall Test Section

WING MODEL

Fig. 12.   Numerical Simulation of 25- by 13-cm Adaptive-Wall Wind Tunnel
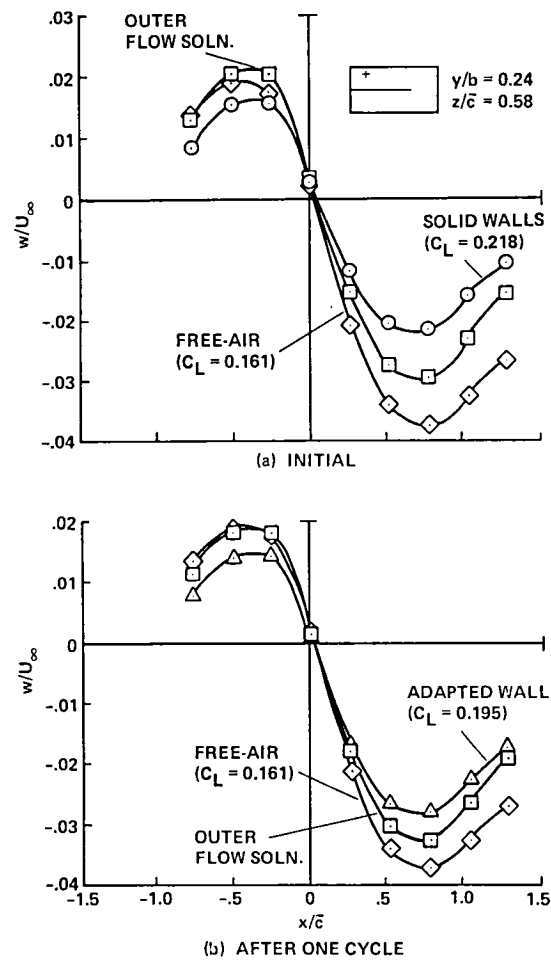
12

Fig. 13. Numerical Simulation: Effect of one Cycle of Adaptive-Wall Procedures
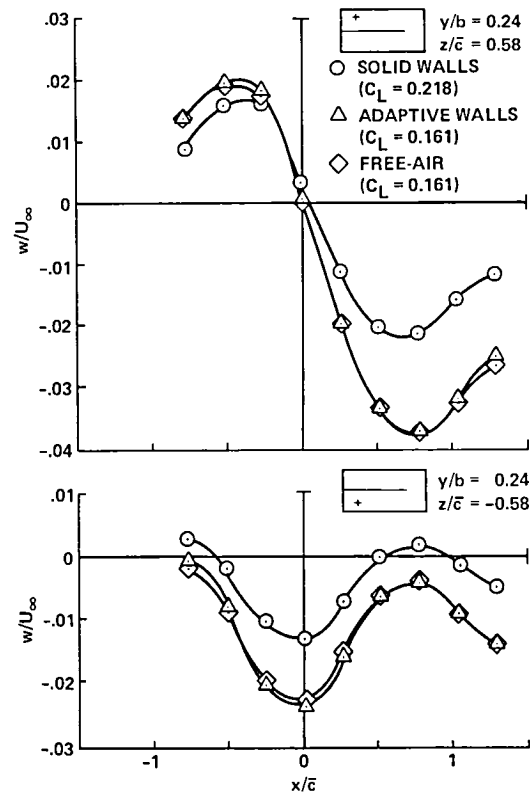
Fig. 14. Numerical Simulation: Effect of Adjusting Top and Bottom Wall Boundary Conditions to Match Free-Air Upwash

1. Report No. NASA TM 84236	2. Government Accession No.	3. Recipient's Catalog No.
4. Title and Subtitle Adaptive Wall Wind Tunnel Research at NASA Ames Research Center		5. Report Date May 1982
		6. Performing Organization Code
7. Author(s) Edward T. Schairer and Joel P. Mendoza		8. Performing Organization Report No. A-8893
		10. Work Unit No. T-3253Y
9. Performing Organization Name and Address NASA Ames Research Center Moffett Field, Calif. 94035		11. Contract or Grant No.
		13. Type of Report and Period Covered Technical Memorandum
12. Sponsoring Agency Name and Address National Aeronautics and Space Administration Washington, D. C. 20546		14. Sponsoring Agency Code 505-31-31

15. Supplementary Notes
Point of Contact: Edward T. Schairer, MS 227-8, Ames Research Center,
Moffett Field, CA. 94035 (415) 965-6116 or
FTS 448-6116

16. Abstract   Adaptive-wall wind-tunnel research conducted at Ames Research Center, NASA, is summarized. This research includes small-scale two-and three-dimensional wind-tunnel experiments and numerical experiments with a three-dimensional adaptive-wall simulator. In the two-dimensional experiment, an NACA 0012 airfoil was tested in a 25- by 13-cm slotted-wall test section. Airflow through the test-section walls was controlled by adjusting the pressures in segmented plenums. Interference-free conditions were successfully attained in subsonic and transonic flows. Based on the design of this small-scale test section, an adaptive-wall test section is being constructed for the 2- by 2-Foot Transonic Wind Tunnel at Ames. For the three-dimensional experiment, the 25- by 13-cm wind tunnel was modified to permit cross-stream wall adjustments. The test model was a semispan wing mounted to one sidewall. Wall interference was substantially reduced at several angles of attack at Mach 0.60. A wing-on-wall configuration was also modeled in the numerical experiments. These flow simulations showed that free-air conditions can be approximated by adjusting boundary conditions at only the floor and ceiling of the test section. No sidewall control was necessary. Typical results from these experiments are discussed.

17. Key Words (Suggested by Author(s)) Adaptive wall Laser velocimetry	18. Distribution Statement Unlimited Subject Category 09		
19. Security Classif. (of this report) Unclassified	20. Security Classif. (of this page) Unclassified	21. No. of Pages 16	22. Price* A01